Crustal Shortening and Extension in the Central Andes: Insights from a Viscoelastic Model

Mian Liu and Youqing Yang

Dept. of Geological Sciences, University of Missouri, Columbia, Missouri

Seth Stein and Eryn Klosko

Dept. of Geological Sciences, Northwestern University, Evanston, Illinois

The Andes resulted mainly from crustal shortening associated with the South America-Nazca plate convergence in the past ~30 Myr. The GPS data indicate 30-40 mm yr^{-1} crustal shortening across the entire Andean mountain belt and no significant extension in the High Andes, but the seismic data show crustal shortening concentrated in the sub-Andean thrust belt at a much lower rate (< 3 mm yr^{-1}) and limited crustal extension in the High Andes with variable directions, and the geological data suggest 10~15 mm yr^{-1} crustal shortening concentrated in the sub-Andean zone and widespread N-S extension since the Pleistocene. We explore these discrepancies using geodynamic models with timescale-dependent rheology. Using a simple viscoelastic-plastic model, we illustrate the relationship between instantaneous crustal motion reflected by the GPS data and long-term crustal shortening in geological records. We simulate the spatial distribution of the Andean crustal shortening in a three-dimensional viscoelastic finite element model. The results show nearly uniform short-term velocity gradients across the Andes, consistent with the GPS data, and concentrated long-term crustal shortening in the sub-Andean thrust zone, consistent with geological observations. Gravitational collapse in the high Andes is shown to be consistent with modern earthquake mechanisms, and the change of topographic loading along the Andes may explain the along-strike variation of extension directions indicated by seismic data. We explore the effects of boundary conditions and basal shear in the model for possible causes of the reported changes in the orientation of crustal extension through the Late Cenozoic.

1. INTRODUCTION

The Andes are second only to the Himalayan-Tibetan plateau as the largest mountain belt on Earth (Fig. 1). The high Andean topography (~4000 m) and the broad (350-400 km) Altiplano-Puna plateau are comparable to the Himalayan-Tibetan topography, but there remains a fundamental difference between these two orogens: the Andes formed in the absence of continental collision or terrain accretion [*Allmendinger*, 1997]. Although numerous factors, including magmatic addition and mantle flow, may have contributed to the Andean mountain building [*Fukao et al.*, 1989; *Russo and Silver*, 1996; *Zandt et al.*, 1996; *Pope and Willett*, 1998], most workers believe that crustal shortening in the past 30 Myr, resulting from the convergence between the subducting Nazca plate and the overriding South American, is the major cause [*Dewey*, 1970; *Isacks*, 1988; *Sheffels*, 1990; *Baby et al.*, 1992a; *Dewey and Lamb*, 1992; *Allmendinger*, 1997]. However, how subduction of an oceanic plate leads to significant crustal shortening and mountain building in the overriding continental plate is not well understood. For example, in the Cascades and the Aleutian trench, similar subduction does not produce major orogens.
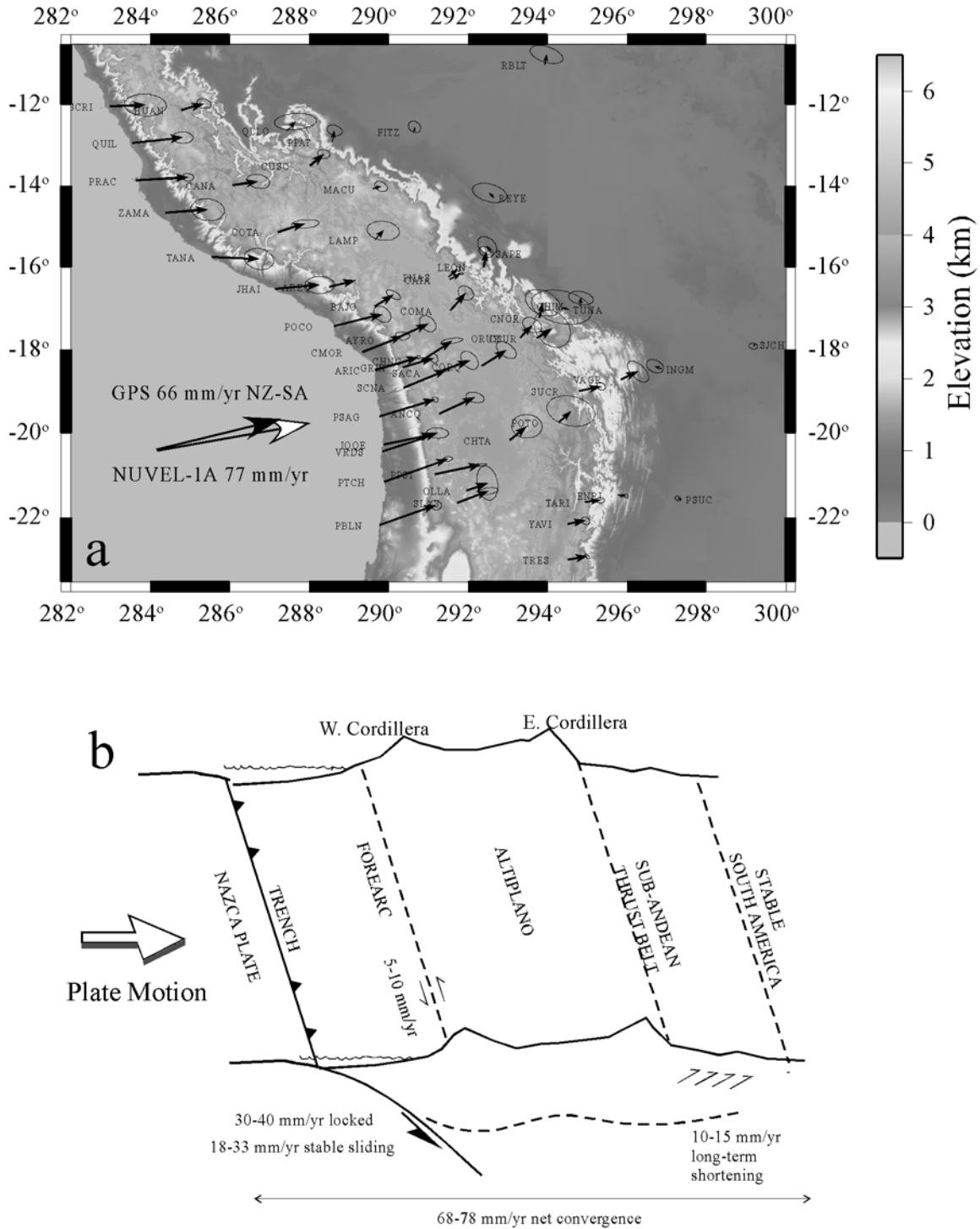
Recent GPS measurements over the Central Andes [*Leffler et al.*, 1997; *Norabuena et al.*, 1998; *Norabuena et*

al., 1999; *Kendrick et al.*, 2001] show present crustal shortening across the Andes. Although the inferred velocity field has reasonable uncertainties due to the short interval of measurements, the pattern seems robust. The GPS results indicate ~66 mm yr^{-1} convergence between the Nazca plate and the stable South America [*Angermann et al.*, 1999; *Norabuena et al.*, 1999] (Fig. 1). This is similar although less than the predictions of the NUVEL-1A plate motion model (~77 mm yr^{-1}) based on marine magnetic anomalies averaged over the past 3 Myr [*DeMets et al.*, 1994]. This discrepancy may reflect the slowing of the plate convergence [*Norabuena et al.*, 1999; *Sella et al.*, 2002], and part of the discrepancy may indicate intraplate shortening shortening within the Nazca plate seaward of the trench [*Yang and Liu*, 2002]. About half of the plate convergence is locked at the plate boundary, causing 25-35 mm yr^{-1} eastward compression across the entire orogen relative to stable South America (Fig. 1). However, the geologically derived average rate of crustal shortening over the past 25 Myr is much lower (8-13 mm yr^{-1}) [*Sheffels*, 1990; *Schmitz*, 1994]. The shortening rate estimated from the seismic moments of earthquakes is even lower (1-3 mm yr^{-1}) [*Suarez et al.*, 1983], although this estimate is a minimum because aseismic slip is not included in the calculations and the sampling period may have missed infrequent very large earthquakes.

The spatial distribution of crustal shortening is also discordant among these different observations. The nearly linear eastward decrease of GPS velocity across the Andes indicates present crustal shortening over the entire Andean mountain belt. However, geological evidence show that, at least for the past few million years, crustal shortening has been concentrated in the sub-Andean fold and thrust belt (FTB) [*Isacks*, 1988; *Sheffels*, 1990], consistent with modern seismicity [*Suarez et al.*, 1983]. *Leffler et al.* [1997] and *Norabuena et al.* [1998] suggested that the GPS velocity in the coastal area and the Altiplano represents elastic strain that will be released in future earthquakes, and only within the sub-Andean FTB does the GPS velocity represent about 10-15 mm yr^{-1} of permanent crustal shortening. This interpretation appears consistent with the geologically derived crustal shortening rate and pattern in the sub-Andean FTB, but it remains unclear why the GPS velocity reflects permanent strain in the sub-Andes and elastic strain in other parts of the mountain belt.

Furthermore, the current GPS data raise the question of whether the High Andes have been collapsing. Geological studies suggest that N-S extension was a predominant feature in the High Andes in the past few Myr [*Dalmayrac and Molnar*, 1981; *Mercier*, 1981; *Dewey*, 1988]. However, the GPS velocity field shows no clear sign of such extension but a nearly uniform E-W compression (Fig. 1). This is in contrast to the Himalayan-Tibetan orogen where the GPS data are consistent with the geologically observed crustal extension roughly perpendicular to convergence [*King et al.*, 1997; *Larson et al.*, 1999; *Chen et al.*, 2000].

In this paper we explore the discrepancy between the geodetic, seismological, and geological data on crustal shortening and extension in the central Andes using geodynamic models that consider timescale-dependent behavior of the lithosphere. It is well known that the rheologic response of the Earth to tectonic forces depends on timescales. Over a short period the Earth behaves nearly as an elastic body, accounting for the transmission of seismic (i.e., elastic) waves. Over the geological timescale of millions of years, however, the Earth creeps by viscous flow [*England and McKenzie*, 1982; *Ranalli*, 1995]. The GPS velocity field across the Andes, measured over a period of a few years, is essentially a snapshot of the instantaneous velocity field including both permanent strains and elastic strains that will be released during future earthquakes or aseismic slip [*Leffler et al.*, 1997; *Norabuena et al.*, 1998; *Dragert et al.*, 2001]. The geological record, on the other hand, reflects only the permanent strains. Here we use a simple plastic-viscoelastic model to illustrate the relationship between the instantaneous crustal shortening reflected in the GPS measurements and long-term crustal shortening indicated by geological observations. We then present a three-dimensional (3-D) finite element model exploring the stress state and crustal deformation in the Andes at different timescales and with various boundary conditions. The model predicts a nearly uniform short-term velocity gradient across the Andes, consistent with the GPS data, and long-term crustal shortening concentrated in the sub-Andean FTB, consistent with the geological evidence. The model results also provide useful insight into crustal extension in the High Andes.

Figure 1. (a) Topography and GPS site velocity relative to stable South America (SA) of the central Andes [*Leffler et al.*, 1997; *Norabuena et al.*, 1998; *Kendrick et al.*, 2001]. Rate scale is given by the NUVEL-1A vector of the Nazca plate (NA) relative to the South American plate. (b) Sketch of a cross-section of the Andean orogen showing velocity distribution inferred from GPS data.

2. WHY ARE THE GPS RATES OF CRUSTAL SHORTENING HIGHER THAN THE GEOLOGICAL RATES?

Norabuena et al. [1998] and *Leffler et al.* [1997] answered this question by suggesting that part of the GPS-measured strain is elastic and will be released by future earthquakes. Transient strain accumulation and release associated with the seismic cycle at subduction zones have been well studied [*Savage*, 1983], but the relationship between the elastic and plastic (permanent) strain and their implications for Andean mountain building are not clear. *Liu et al.* [2000a] illustrated the relationship between long-term and short-term crustal shortening across both the subduction zone and the Andes using a simple plastic-viscoelastic model containing a dashpot, a spring, and a pair of frictional plates (Fig. 2a). The first two parts represent a viscoelastic (Maxwell) body, and the frictional plates represent faults, although in this simple model the only fault we consider is the thrust interface at the trench. This system provides a first-order approximation of the mechanical behavior of the Andean crust: mainly elastic over short periods, viscous over long timescales, and plastic (sliding along the subduction zone) when tectonic stresses exceed the threshold for seismic or aseismic slip at the subduction zone. When part of the plate convergence is locked at the trench and causes compression at the western edge of the Andean crust, simulated here by compression at the leading edge of the system at a constant velocity V_o, the stress increases till it reaches some yield limit (σ_y), then sliding (an earthquake) occurs between the frictional plates, stress drops to a background value σ_b, and the process repeats (Fig. 2b). The stress is uniform within the system: $\partial\sigma / \partial x = 0$, whereas its time-dependent evolution can be derived from integrating the constitutive equation of a Maxwell body:

$$\dot{\varepsilon} = \dot{\sigma}/E + \sigma/\eta \qquad (1)$$

with boundary conditions: $u(x=w,t)=0$ and $u(x=0,t)=V_0 t$, and initiation conditions: $u(x,t=0)=0$ and $\sigma(x,t=0)=\sigma_b$. Here $\dot{\varepsilon}$ and $\dot{\sigma}$ are the time-derivatives of strain and stress, respectively; E is the Young's modulus, η is the viscosity, and u is the displacement. The result is

$$\sigma(t) = \sigma_m - (\sigma_m - \sigma_b)\exp(-t/\tau) \qquad (2)$$

where $\sigma_m = \eta V_0 / W$ is the theoretical stress limit of the system and $\tau = \eta / E$ is the Maxwell time. The displacement during earthquakes is $\Delta u = W\Delta\sigma / E$, and the time-interval for earthquakes is $\Delta t = \tau \ln(1 + \Delta\sigma /(\sigma_m - \sigma_y))$, where $\Delta\sigma = \sigma_y - \sigma_b$ is the stress drop during earthquakes. The averaged long-term shortening rate of the system, V_c, is lower than, but related to V_o:

$$\begin{aligned} V_c &= V_0 - \Delta u / \Delta t \\ &= V_0 - W\Delta\sigma /\eta \ln(1 + \Delta\sigma /(\sigma_m - \sigma_b)) \end{aligned} \qquad (3)$$
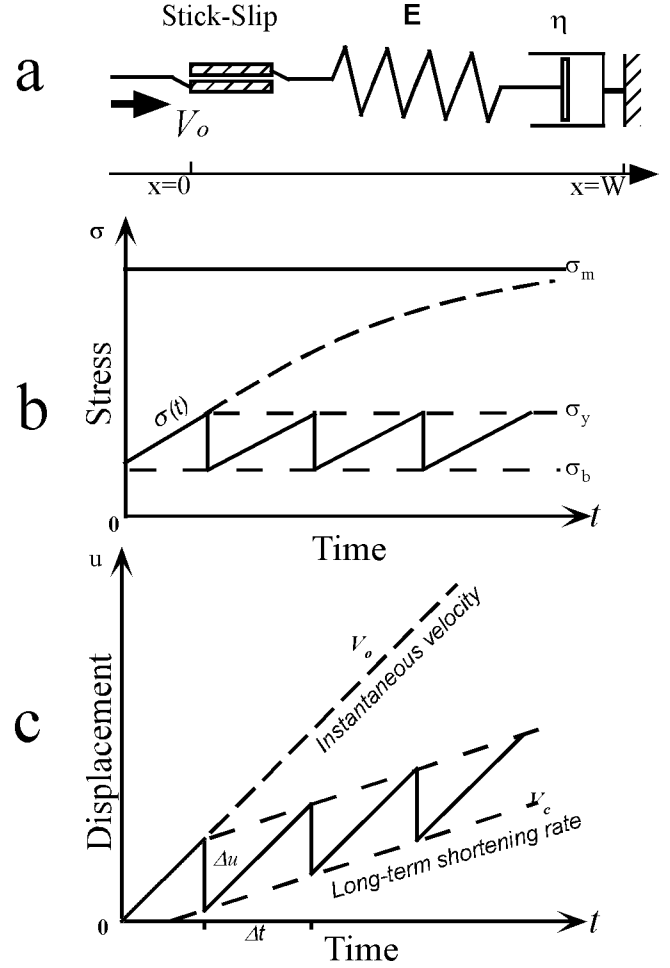
Figure 2. (a) Analog model for a plastic-viscoelastic South America plate. The frictional plates model the effects of the earthquake cycle at the trench whereas the dashpot and the spring together make a viscoelastic (Maxwell) body that has both viscous flow leading to permanent deformation and elastic strain that will be recovered by earthquakes (sliding of the frictional plates). (b) Stress evolution for the viscoelastic-plastic system. Symbols are explained in text. (c) Displacement history showing the relationship between instantaneous velocity and long-term velocity of

permanent shortening at the left end of the viscoelastic-plastic system. Displacement accumulates at the instantaneous rate V_o except during sliding (earthquake) events, when a rebound Δu occurs. The GPS data would record a velocity gradient starting at V_o from the trench, whereas the envelope of the displacement curve V_c is the long-term shortening rate reflected in geological records.

For $\Delta\sigma << (\sigma_m - \sigma_y)$, (3) can be simplified to $V_c = W\sigma_y / \eta$. When the shortening is uniformly distributed across the system, V_c / W is the long-term, averaged strain rate: $V_c / W = \dot{\varepsilon}_a = \sigma_y / \eta$. In other words, the averaged long-term deformation of this plastic-viscoelastic system is essentially that of a viscous fluid. The relationship between the instantaneous and the long-term shortening rate of the system is shown in Fig. 2c.

Applying the model to the Andes, we take the instantaneous velocity, V_o, to be the GPS velocity near the trench, which is 30-40 mm yr^{-1}. The long-term crustal shortening in the Andes, however, is that represented by V_c, which is 10-15 mm yr^{-1} [*Sheffels*, 1990]. Note that in this simple model V_c does not depend strongly on the instantaneous crustal shortening rate V_o because of the self-regulation of the system. A higher V_o may cause more frequent (or greater) earthquakes but not a higher long-term shortening rate. The long-term crustal shortening is mainly a function of the viscosity and the initial width of the system, which may represent the weak zone over which the Andes developed [*Isacks*, 1988]. It is important to note that V_o represents the portion of the interplate convergence rate that is locked at the subduction zone thrust fault and hence available to deform the overriding plate. This fraction of the convergence may have varied with time, as suggested by the observation [*Hindle et al.*, 2002] that the rate of permanent crustal shortening in the foreland thrust belt (V_c in this formulation) has increased over the past 10 Ma although plate convergence has been slowing [*Somoza*, 1998; *Norabuena et al.*, 1999; *Sella et al.*, 2002].

3. WHAT IS THE SPATIAL DISTRIBUTION OF ANDEAN CRUSTAL SHORTENING?

The nearly linear GPS velocity gradient across the Andes (Fig. 1) indicates a uniform distribution of crustal shortening over the entire Andes, in contradiction to the geological and seismological evidence of concentrated crustal shortening in the sub-Andean FTB. This discrepancy may also be attributed to timescale-dependent rheol-

ogy of the Andean crust. In this section we discuss the short-term and long-term crustal deformation in the Andes simulated in a three-dimensional finite element model.
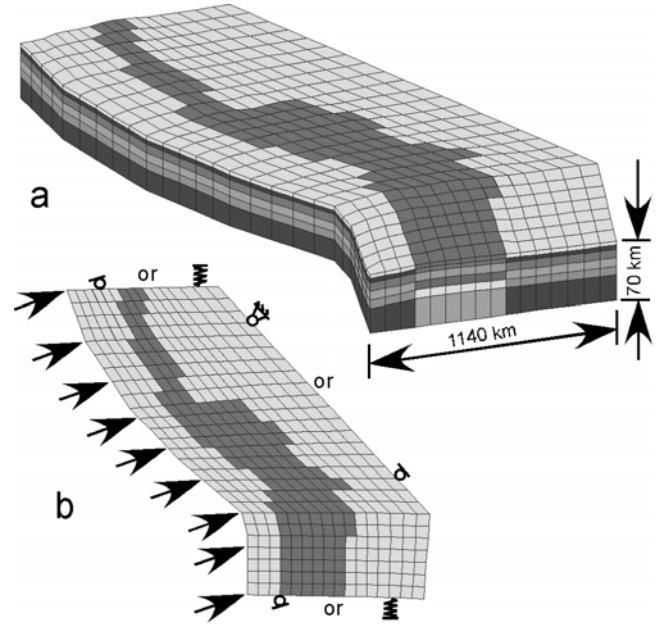
Figure 3. (a) Finite element mesh of the three-dimensional viscoelastic model. Dark areas are the Andean orogen. Digital topography of the Andes is used to calculate the gravitational buoyancy force of the orogen. The model has six layers with variable viscosity approximating the typical strength profile of the lithosphere (see Fig. 4). (b) General boundary conditions. The velocity imposed on the western margin is either the GPS velocity near the trench or the long-term geological rate of crustal shortening. On the northern and southern sides either rollers or springs are used. The rollers restrict displacement in the direction of plate convergence, to be consistent with the GPS velocity field; the springs allow along-strike movement of crustal material under lateral mechanical equilibrium. The eastern side is fixed in most cases except in a few experiments where rollers are used to allow along-strike motion only.

Fig. 3 shows the numerical mesh and the general boundary conditions of the model. The major driving force for Andean mountain building is assumed to be crustal shortening associated with plate convergence, which is simulated by the imposed velocity at the western edge of the South America. The tectonic compression is largely balanced by the gravitational potential arising from the isostatically supported elevation of the mountain ranges [*Dalmayrac and Molnar*, 1981; *Molnar and Lyon-Caen*, 1988], which is calculated in the model from the digital topography assuming a constant crustal density of 2800 kg m^{-3}. The lateral boundaries are specified by velocity boundary conditions: a displacement boundary along the western edge of the

model and a fixed or "roller" condition along the eastern side reflecting no crustal shortening within stable South America. On the northern and southern boundaries either a roller condition is used to restrict displacement to the direction of plate convergence, or a spring condition is used to allow material flow along the strike of the mountain belt. The elastic parameters used in the calculations include the Young's modulus (7×10^{10} MPa) and the Poisson's ratio (0.25). Winkler springs are used to simulate the body forces induced by vertical displacement of density boundaries and the isostatic restoring force at the base of the model crust [*Desai*, 1979; *Williams and Richardson*, 1991].

Viscosity (10^{22} Pa s)
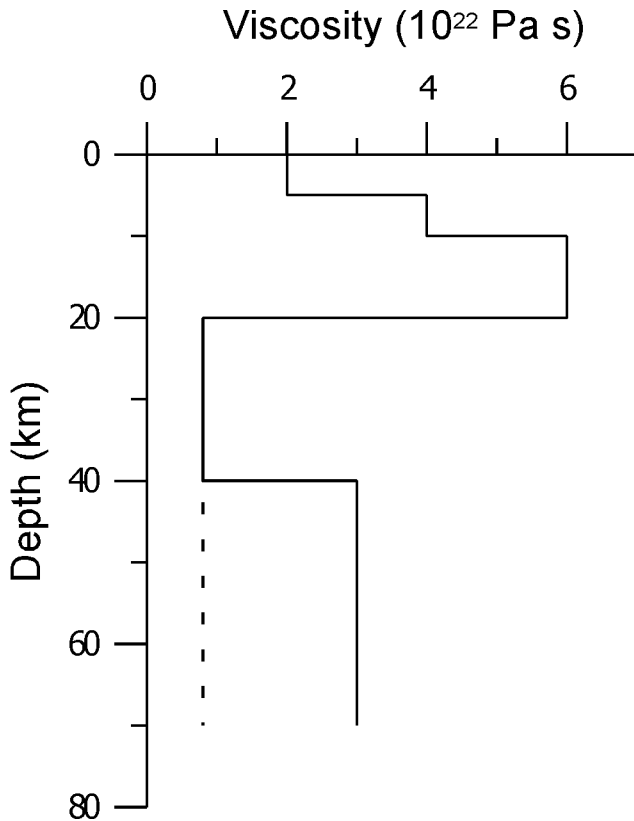
Figure 4. A typical profile of the effective viscosity used in the model lithosphere. The solid profile is for the lowland, and the dashed profile is for the mountain belt. The two profiles overlap above 40 km depth.

The rheology of the model lithosphere is taken to be viscoelastic. Although the viscous creep of the lithosphere is nonlinear [*Goetze and Evans*, 1979; *Kirby and Kronenberg*, 1987], an effective viscosity, which is a function of the strain rate in addition to the temperature and pressure, can be used in the viscoelastic model [*Ranalli*, 1995]. The model lithosphere (defined here as the mechanical boundary layer) is 70 km thick and has six layers with variable

effective viscosity to approximate the typical strength profile of the continental lithosphere (Fig. 4).

Short-Term Velocity
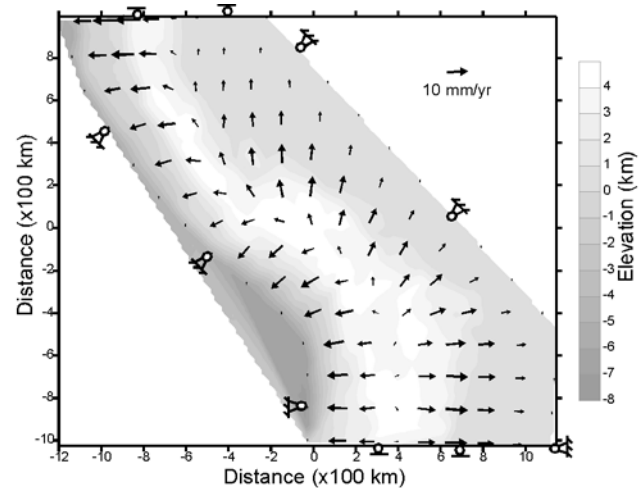
Long-Term Velocity
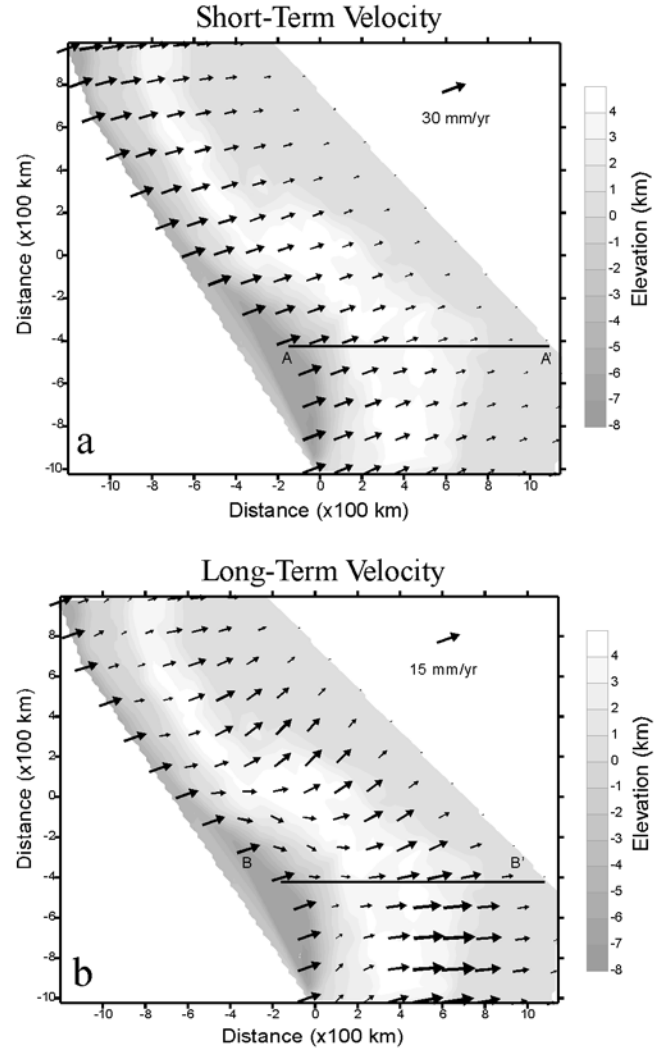
Figure 5. (a) Predicted surface velocities across the Andes for short-term crustal deformation. Scale is shown in the upper right corner. Solid line (A-A') indicates the location of the velocity profile in Fig. 7. (b) Predicted surface velocities for long-term crustal deformation. The non-uniform velocity gradients across the Andes are caused by gravitational spreading (Fig. 6) superimposed on the deformation field resulting from tectonic compression on the western boundary. Solid line (B-B') indicates the location of velocity profile in Fig. 7. See text for the boundary conditions in (a) and (b).

The near-elastic behavior of the Andean crust at a short time scale ($<10^2$ yr) can be simulated with an extremely high viscosity (10^{25}-10^{27} Pa s) of the various crustal layers (Fig. 5a). In this case deformation is dominated by elastic strain while viscous strain becomes negligible. A velocity boundary condition ranging from 32 to 35 mm yr^{-1} with

respect to stable South America was imposed on the western side of the model. This velocity boundary condition, based on the GPS data [*Leffler et al.*, 1997; *Norabuena et al.*, 1998], reflects the fact that only about half of the plate convergence appears to be locked at the interface and hence cause both elastic and permanent deformation of the overriding plate. The small velocity variations imposed on this boundary result from scaling with the model width to avoid introducing artificial internal distortion because of the simplified model geometry. Fig. 5a shows the predicted short-term velocity field across the Andes. The nearly uniform velocity gradient decreasing from the west across the entire Andes to stable South America is similar to the GPS velocity field (Fig. 1).

To simulate the long-term crustal shortening in the Andes, we take the viscosity of various crustal layers to be in the range of 10^{22}-10^{23} Pa s, values assumed appropriate for long-term continental deformation [*England and McKenzie*, 1982; *Lamb*, 2000]. A velocity boundary condition of 10-12 mm yr^{-1} is applied to the west side of the model, as suggested by the geologically averaged shortening rates [*Sheffels*, 1990; *Schmitz*, 1994]. This velocity boundary condition implies that 10-20% of plate convergence is translated into permanent shortening of the overriding plate. We model the displacement field for a period of a few Myr. This time interval is much greater than the Maxwell relaxation time (<0.05 Myr for the model rheology), so viscous strain becomes predominant while elastic strain is negligible. The resultant velocity field shows significant non-uniform gradients across the Andes, in contrast to short-term crustal deformation (Fig. 5b). This difference results from gravitational spreading of the mountain belt, which is negligible for short-term (near elastic) deformation but becomes effective over the long geological time scales (low effective viscosity). While crustal shortening associated with plate convergence pushes the crustal material eastward, gravitational spreading moves the crustal material to both sides of the mountain belt and from the High Andes to the lowland (Fig. 6). Over the Eastern Cordillera and part of the Altiplano, the eastward velocity due to compression at the plate boundary is amplified by gravitational spreading in the same direction, causing the velocity peak over this region (Fig. 5b). The large decrease of velocity across the sub-Andean zone indicates concentrated crustal shortening, consistent with geological and seismological observations. The long-term velocity in the Western Cordillera is relatively low, because there gravitational spreading is in the direction opposite (westward) to the eastward tectonic compression. This is clearer in regions

south of the bend near 18°S. North of the bend, there is a large component of northward flow driven by gravitational spreading, causing a counter-clockwise rotation of the velocity vectors (see Fig. 5b).

Figure 6. Predicted surface velocity field due only to gravitational spreading of the Andes. Rollers are applied to all boundaries. The arrow in the upper right corner shows the velocity scale.

Fig. 7 compares the predicted short-term and long-term velocity field with the GPS velocity. The GPS velocity gradient is nearly linear (linear correlation coefficient R = 0.87), which can be reasonably well fit when the vertically averaged effective viscosity of the model lithosphere is >10^{24} Pa s. The effects of gravitational spreading diminish quickly when the averaged viscosity becomes greater than 10^{25} Pa s, so the elastic strain predominates. Although Fig. 7 clearly shows that the GPS data can be best fit with a nearly elastic rheology, there are some slight rotations of the GPS velocity vectors just north of the bend of the orogen (Fig. 1a) that bear some resemblance to the velocity field in Fig. 5b. The sparse GPS sites and the present uncertainties of the GPS velocities do not allow more meaningful comparison. If these rotations are real, then perhaps the overall rheology of the lithosphere over the timescale pertinent to the GPS measurements is close to be elastic but is viscous enough to allow noticeable effects of gravitational spreading. In the following we show that the boundary conditions will also have important impacts on the predicted velocity field.
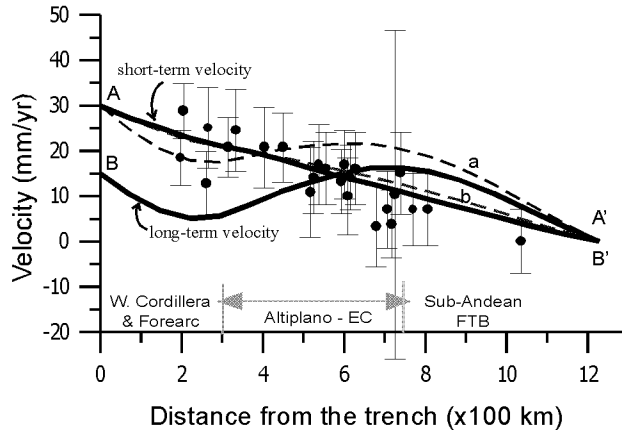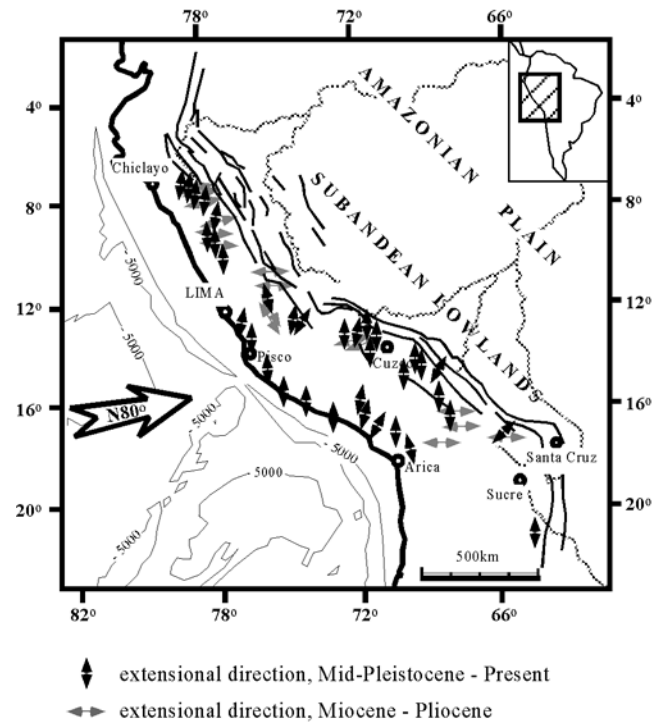
Figure 7. Comparison of the predicted short-term and long-term crustal deformation across the Andes with GPS velocity data [*Norabuena et al.*, 1998]. Curves A-A' and B-B' are the short-term and long-term velocity from Fig. 5a and Fig. 5b, respectively. Dashed curve a is for the same rheology structure as for B-B' but with the velocity boundary condition same as those for short-term deformation (line A-A'). Dashed curve b shows the lower limit of viscosities (1-6 × 10^{24} Pa s) for simulating short-term deformation. Below this limit significant non-uniform velocity gradient would result.

4. ARE THE ANDES COLLAPSING?

Many large orogenic belts in the world experienced synorogenic extensional collapse [*Dewey*, 1988; *Molnar and Lyon-Caen*, 1988; *Hodges and Walker*, 1992; *Liu et al.*, 2000b]. In the Himalayan-Tibetan plateau, for example, E-W crustal extension has been a dominant feature in the past ~10 Myr, although the plate convergence has continued at a nearly constant rate of ~40-50 mm yr^{-1} during this period [*Molnar and Chen*, 1983; *Armijo et al.*, 1986; *DeMets et al.*, 1994; *Yin and Harrison*, 2000]. The evidence for crustal extension in the High Andes, however, is less clear. *Mercier et al.'s* [1992] analysis of faulting history in the central Andes finds that Late Cenozoic crustal extension was widespread and changed from mainly E-W to mainly N-S since Pleistocene (Fig. 8). Other studies have found roughly N-S extension near the northern and southern ends of the Altiplano-Puna plateau [*Suarez et al.*, 1983; *Sebrier et al.*, 1985]. The focal mechanisms of normal-faulting earthquakes in the Altiplano show some evidence for present extension [*Dalmayrac and Molnar*, 1981; *Grange et al.*, 1984] (Fig. 9). However, there is no clear sign of crustal extension from the current GPS data (Fig. 1): the velocity vectors are nearly parallel to plate convergence and the magnitude decreases smoothly from the coastal region to the sub-Andean zone, indicating predominant E-W compression.

Figure 8. Geologically indicated crustal extension in the central Andes. Black arrows are sites of recent (Pleistocene - present) extension, and gray arrows are older (Miocene - Pliocene) extensions. After *Mercier et al.* [1992].

Are the Andes collapsing? We have argued that the GPS velocity field, measured over a few years, may not accurately represent the long-term strain patterns, whereas focal mechanism of moderate events averaged over decades typical reflect long-term strain rate and thus steady-state stress field [*Holt and Haines*, 1993; *Flesch et al.*, 2001]. To investigate the long-term stress pattern in the Andes, we conducted systematic numerical experiments using the three-dimensional viscoelastic model described in Fig. 3. The effective viscosity of the various layers of the model lithosphere is taken to be in the range of 10^{22}-10^{23} Pa s, values appropriate for continental deformation over geological time scales. Transient stress accumulation and release associated with earthquakes are ignored. This numerical model is similar to the viscous thin-shell model [*England and McKenzie*, 1982] but is three-dimensional with the effective viscosity varying with depth and between the mountain belts and the lowland.

Fig. 10 shows the predicted steady-state stress pattern within the upper crust. The boundary conditions and model parameters are the same as those in Fig. 5b. The three-dimensional stress state is shown by the stereographic

lower-hemisphere projection similar to that used in earthquake focal mechanism solutions. The predicted stresses are predominately compressional in the forearc and the sub-Andes but extensional in the High Andes. The extensional direction changes from mainly E-W south of the bend near 18°S to roughly N-S just north of the bend, and back to E-W in regions north of 12°S. This pattern is generally consistent with the earthquake focal mechanisms (Fig. 9). Notice that the stresses shown here are deviatoric stresses. In the forearc and sub-Andes the horizontal stress σ_{xx} is much greater than the vertical stress σ_{zz}, resulting in large deviatoric stresses. In contrast, under the High Andes the magnitude of σ_{xx} is similar to that under the lowland, but σ_{zz} becomes slightly greater than σ_{xx}, leading to the tensional deviatoric stresses there with relatively small magnitudes. Fig. 10b shows the depth-variation of the stress state along the A-A' profile in Fig. 10a. As in Fig. 10a, the 3-D stress state at each point is shown by a stereographic lower-hemisphere projection, but we now look at the stress variations with depth. Under the forearc and sub-Andean zone the stress state predicts predominately thrust faults, with σ_3 nearly vertical and σ_1 oriented NE-SW and nearly horizontal along this profile. Under the High Andes the stress state predicts normal faults. The magnitude of stresses changes with depth because of the depth-dependent effective viscosity in the model (Fig. 4). The relatively low stresses in the lower crust are caused by viscous relaxation [*Liu et al.*, 2000b].

The predicted pattern of extensional stresses in Fig. 10 reflects the control of topography of the Andes: crustal material tends to flow from highland to lowland. Whereas this stress pattern is consistent with that indicated by modern earthquakes, geological evidence from newly formed faults shows predominantly N-S extension [*Mercier et al.*, 1992; *Allmendinger*, 1997]. Many of the extensional faults are found near the northern end of the Altiplano plateau [*Sebrier et al.*, 1985; *Allmendinger et al.*, 1989; *Cladouhos et al.*, 1994], which would be consistent with Fig. 10a. However, if the recent N-S extension is more widely spread, such as those near the northern end of the Andes (Fig. 8), other explanations may be needed. Using the displacement field based on Kley's [1999] reconstruction of balanced cross-sections, *Hindle et al.* [2002] calculated the geologically averaged finite strain rate field and showed that it is remarkably consistent with the GPS data. In other words, there is no indication of finite along-strike extension, so the N-S extension may be local phenomena that could result from differential crustal shortening. However, given the paucity of geologic data for recent crustal exten-

sion and the long time interval in *Hindle et al.*'s reconstruction, orogenwide N-S extension may not be excluded. In such case we need to explore the boundary conditions used in our model. In Fig. 10 we used rollers on the northern and southern sides to restrict displacement in the direction of plate convergence, to be consistent with the GPS data. This is a strict condition that prohibit along-strike motion of crustal material. Relaxing this condition by replacing the rollers with spring elements, i.e., allowing along-strike crustal movement under the condition of steady state lateral mechanical equilibrium, the model predicted widespread N-S crustal extension (Fig. 11) that is more consistent with *Mercier et al.*'s [1992] geological data (Fig. 8).
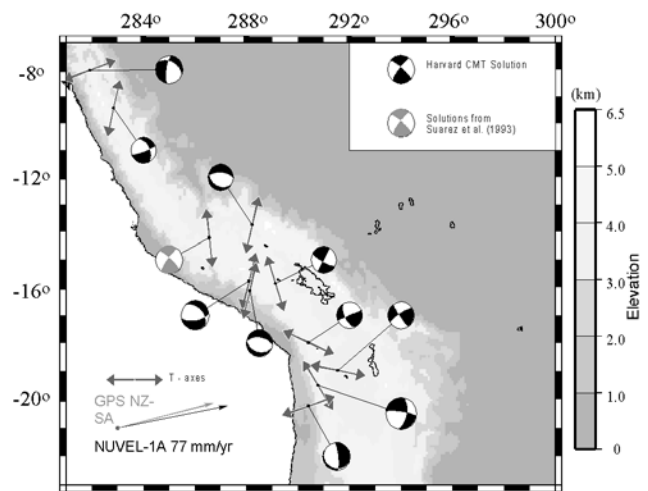
Figure 9. Selected earthquake focal mechanism solutions showing crustal extension in the central High Andes. The T-axes, which bisect the shaded quadrants and represents the least compress principal axes, are projected onto the surface.

Mercier et al. [1992] showed that, from the Miocene to Pliocene, crustal extension in the Andes was dominantly E-W oriented (see Fig. 8), and suggested trench retreat as the cause. Realizing that this mechanism would require the entire overriding plate, including the sub-Andean zone, to be under extension, *Mercier et al.* found some evidence of extension in the sub-Andes and the Pacific lowlands but admitted that these pieces of evidence, especially those from the sub-Andes, are questionable. Because Late Oligocene to Late Miocene (25-7 Ma) is the period of major mountain building in the Andes [*Isacks*, 1988; *Allmendinger*, 1997], a persistent trench retreat is unlikely. An alternative explanation for a widespread E-W extension in the Andes might be a stronger basal shear. Because the gravitational buoyancy force of the Andes is balanced by tectonic compression on the edge of the plate and shear

stresses at its base, increasing basal shear tends to reduce the compressional stresses required at the western margin of the South America plate, and thus facilitate E-W extension within the upper crust. Fig. 12 shows the resulting stress pattern within the upper crust when a 30 MPa basal shear stress is applied to the western half of the model lithosphere while other model parameters including the western velocity boundary condition are the same as in Fig. 10. Comparing the results with Fig. 10, the major effects of basal shear are shown by the enhanced E-W extensional stresses in the western Cordillera and part of the Altiplano. The applied basal shear also enhances crustal compression in the sub-Andes. This scenario would be more consistent with geological observations of concentrated crustal shortening in the sub-Andes [*Sheffels*, 1990; *Baby et al.*, 1992b].

A problem with invoking stronger basal shear under the central Andes before the Pliocene is the lack of clear geological evidence. The central Andes are currently overriding a "normal" subducting Nazca slab (dipping at ~30°). Widespread Neogene volcanism in this part of Andes indicates normal subduction during this period, although the concentration of recent volcanism in the western Cordillera [*James*, 1971; *Allmendinger*, 1997] may indicate steepening of the subducting slab in the past few million years. On the other hand, the required basal shear need not have occurred directly beneath the central Andes; increased basal shear in the adjacent segments of the Andes overriding a flat subducting slab and especially subduction of the Nazca and the J. Fernandez ridges could have helped to release compressional stresses on the western edge of the central Andes.

5. DISCUSSION

The earth has variable rheology at different timescales [e.g., *Ranalli*, 1995]: it behaves elastically over a very short timescale (seconds to hours), but deforms by viscous flow over long timescales ($>10^6$ year). However, lithospheric rheology at timescales between these extremes is not well understood and is likely to vary with spatial scales. Many recent studies of lithospheric rheology and its dependence on time and space scales have been prompted by space-based geodetic measurements that differ from geological observations [*Donnellan et al.*, 1993; *Bourne et al.*, 1998; *Roy and Royden*, 2000b; *Roy and Royden*, 2000a; *Wernicke et al.*, 2000; *Sella et al.*, 2002]. The discrepancies between geodetic strain and seismic data at convergent plate boundaries [*Sbar*, 1983] may also be explained by the different timescales [*Wang*, 2000]. Here we have shown that the apparently discordant observations of crustal shortening

and extension in the central Andes from the GPS, seismological, and geological data can be reconciled by considering the timescale-dependent mechanical behavior of the Andean crust.

The uncertainties in the velocity field derived from the present GPS data are large enough to allow alternative interpretations of a nonuniform distribution of crustal shortening across the Andes [*Leffler et al.*, 1997; *Norabuena et al.*, 1998; *Kendrick et al.*, 2001] or limited crustal extension. A longer interval of measurements would reduce the uncertainties sufficiently to resolve these issues. Nonetheless, the significant discrepancies between GPS and geological rates and distribution of crustal shortening in the Andes would remain and be consistent with the general model proposed here. We note that although the discrepancies between geodetic and geological rates of crustal deformation at many places may be explained by the timescale-dependent rheogy of the continental lithosphere, the relationship between the short-timescale and long-timescale deformation may vary with different tectonic settings. These differences may be due both to the effects of the seismic cycle [*Norabuena et al.*, 1998; *Larson et al.*, 1999; *Bevis et al.*, 2001] and transient aseismic deformation [*Wernicke et al.*, 2000]. This work also provides some independent constraints on the lithospheric rheology for deformation at both short time-scales and long timescales. *England and McKenzie* [1982] have shown that continental deformation over geological timescales can be approximated as that of a flowing thin viscous sheet. However, the effective viscosity of the viscous sheet (i.e., the lithosphere) is poorly known. The viscosity of the sublithospheric mantle, which is inferred from glacial rebound studies to be in the range of 10^{20}-10^{21} Pa s [*Cathles*, 1975; *Lambeck*, 1993], may provide a lower limit to the lithospheric rheology. The upper limit used in various models ranges from the average mantle viscosity (10^{20}-10^{22} Pa s) to infinity (elastic lithosphere). Realizing the problems of lithospheric rheology, *England and McKenzie* [1982] parameterized the vertically averaged effective viscosity of the lithosphere in terms of the Argand number, essentially the ratio of gravitational buoyancy force within the lithosphere and the viscous resistance. Although the Argand number has proven useful for exploring the general patterns of continental deformation, many large-scale tectonic problems require knowledge of the lateral and depth-dependent variations of the lithospheric rheology. Previous estimates of the vertically averaged lithospheric effective viscosity include studies from lithospheric flexure and strain distributions [*Walcott*, 1970; *Lowry and Smith*, 1995; *Flesch et al.*, 2000], with values in

the range of 10^{22}-10^{23} Pa s. Our modeling results imply that the effective viscosity of the Andean lithosphere for long-term deformation must be <10^{23} Pa s. For higher values the predicted extension in the High Andes would be replaced by strike-slip and thrust faulting. Conversely, the effective viscosity of the Andean crust proper for short-term deformation should be > 10^{24} Pa s, because lower values cause significant misfits between the predicted and the GPS velocity fields (Fig. 7).
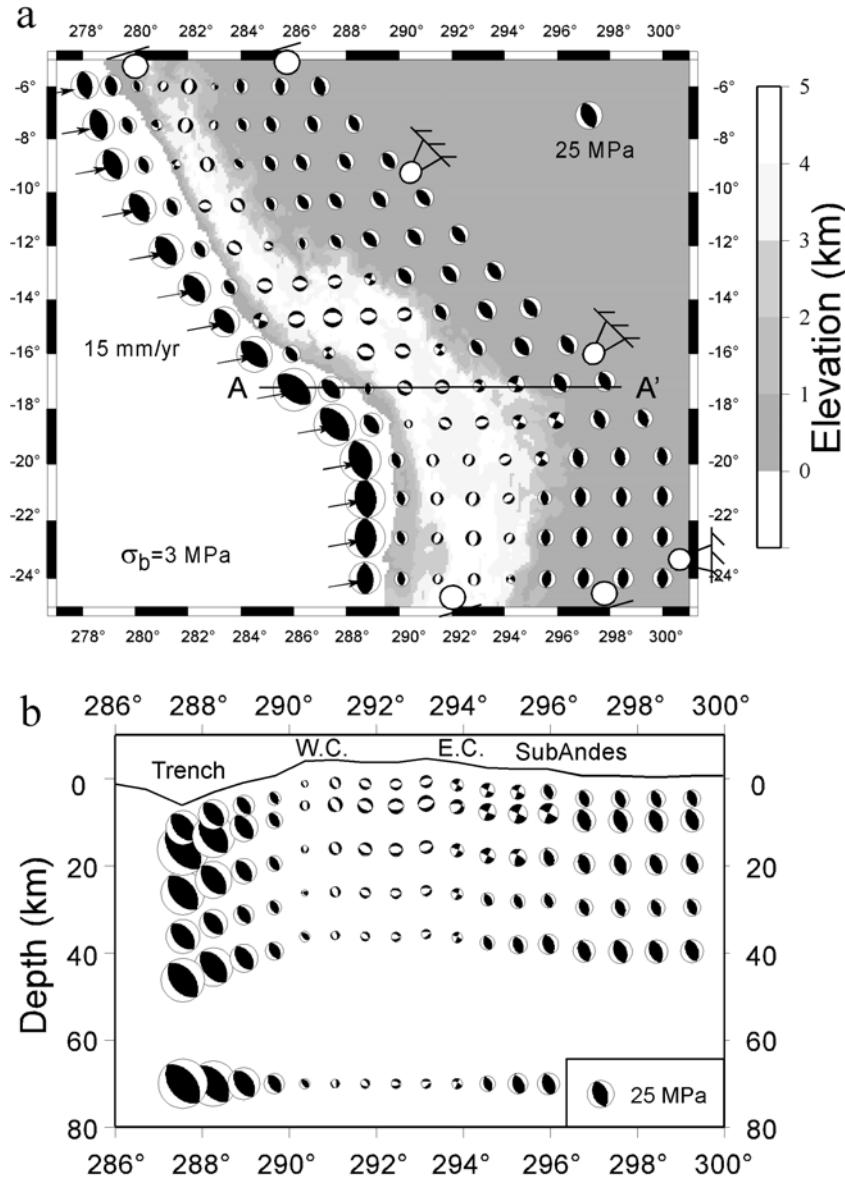
Figure 10. (a) Predicted steady-state deviatoric stresses within the upper crust at 10 km depth. The three-dimensional stresses are shown by the stereographic lower-hemisphere projection similar to that used in earthquake focal mechanism solutions. The maximum (σ_1) and minimum (σ_3) principal stresses bisect the white and shaded quadrants, respectively, and are similar to the P- and T- axes in earthquake focal mechanisms. The stress states are compressional in the forearc and sub-Andes but extensional in the High Andes. The along-strike variation of the extensional directions is consistent with that indicated by earthquakes (Fig. 9). The line A-A' shows the location of the vertical section in (b). The stress symbols are scaled by magnitude with the scale shown in the upper right corner. σ_b is the basal shear applied to the western half the model base. The arrows, rollers, and hinges show the boundary conditions. The deviatoric stresses near the trench are capped at 50 MPa in the figure for clear visualization although the values can be greater. The same is done for Figs. 10b, 11 and 12. (b) Stress variation in a depth-section along profile A-A' in (a). As in (a), the 3-D stress state at each point is shown using the lower-hemisphere stereographic projection. Vertical exaggeration is 10:1. Scale is shown in the lower right corner.
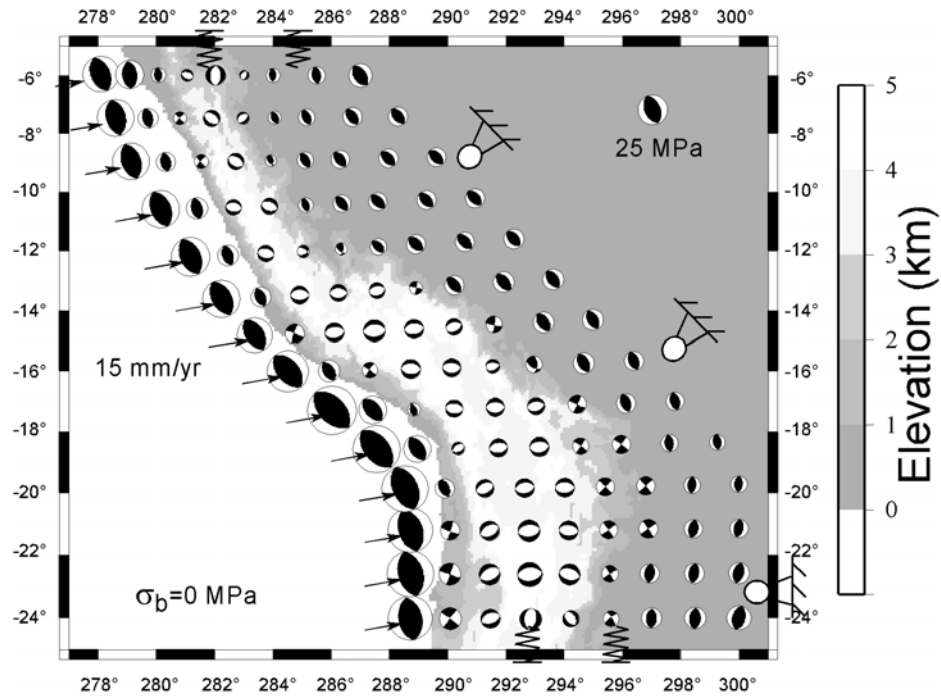
Figure 11. Predicted steady-state deviatoric stresses in the upper crust (at 10 km depth) with spring boundary conditions on the northern and southern sides. Other parameters and symbols are the same as in Fig. 10. N-S extension in the High Andes is enhanced in this case.
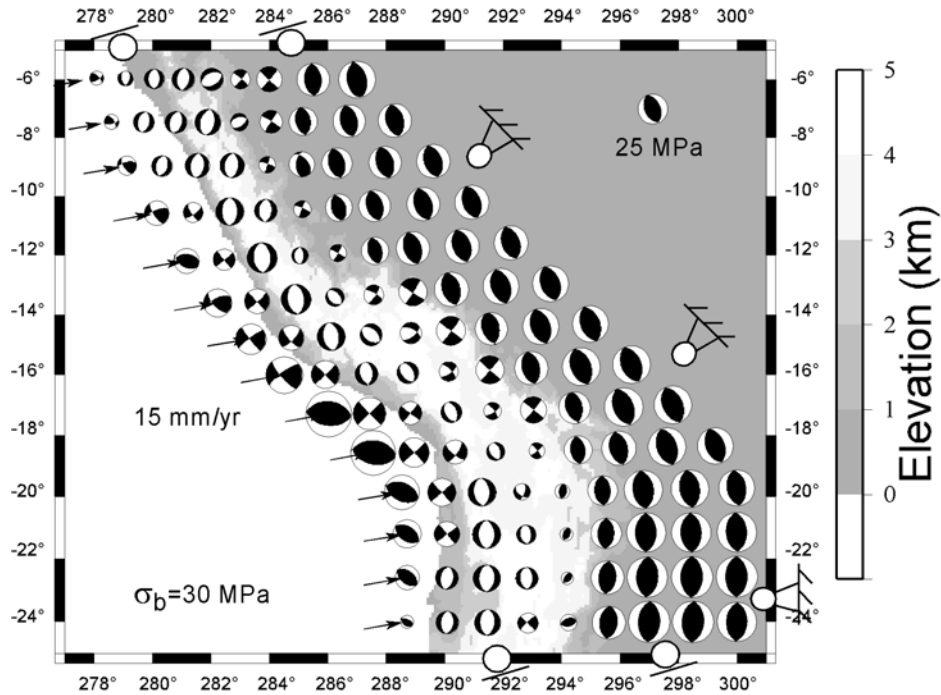
Figure 12. Predicted steady-state deviatoric stresses in the upper crust (at 10 km depth) with a strong basal shear. Model parameters are the same as in Fig. 10, except that a 30 MPa eastward shear stress is applied to the base of the western half of the model lithosphere. Note the enhanced E-W extension in western Cordilleran and part of the Altiplano, and enhanced compressional stresses in the sub-Andes.

6. CONCLUSIONS

1. The discrepancies among geodetic, seismological, and geological estimates of the rates and distribution of crustal shortening in the central Andes can be reconciled by the timescale-dependent rheology and mechanical behavior of the continental lithosphere.

2. The GPS velocity field in the Andes reflects instantaneous crustal shortening that includes both permanent strains and elastic strains due to the seismic cycle that will be recovered during future earthquakes or aseismic slip, whereas the geological rate of crustal shortening represents only the permanent strain and is therefore lower than the GPS rate. The relationship between the long-term and short-term shortening rates can vary with different tectonic settings. The long-term crustal shortening rate depends on the effective viscosity of the Andean lithosphere and the fraction of plate convergence locked at the trench for driving crustal shortening.

3. In our model, the short-term deformation of the Andean crust as reflected in the present GPS data can be well matched with that of an elastic lithosphere or a litho-sphere of high ($>10^{24}$ Pa s) effective viscosity. At short timescales gravitational spreading of the Andean orogen is insignificant, so crustal deformation is controlled by the forces acting on the plate boundaries. This effect explains the nearly uniform GPS velocity gradient across the Andes. Over long geological time scales, viscous deformation becomes predominant. The long-term deformation of the Andes is consistent with the effective viscosity of all lithospheric layers being less than 10^{23} Pa s. Gravitational spreading of the orogen becomes significant for the long-term deformation. The long-term averaged rate of crustal shortening on the western margin of the South America plate is much lower than the short-term rate. In the sub-Andes the direction of gravitational spreading coincides with that of crustal shortening associated with plate convergence, resulting in the concentrated crustal shortening there.

4. Active crustal extension in the High Andes indicated by seismic data is consistent with gravitational collapse. The along-strike variation of extensional directions can be attributed to the variable topography. Widespread N-S extension as suggested by some interpretations of structural geologic data may be predicted using non-rigid boundary conditions on the southern and northern sides in the model. Strong basal shear tends to enhance both E-W extension in the High Andes and crustal shortening in the sub-Andes. This effect may have contributed to the predominant E-W extension in the Andes between Miocene and Pliocene, but the evidence supporting a stronger basal shear during that time period is not clear.

REFERENCES

Allmendinger, R.W., M. Strecker, J.E. Eremchuck, and P. Francis, Neotectonic deformation of the southern Puna Plateau, northwestern Argentina, *J. South Am. Earth Sci.*, *2*, 111-130, 1989.

Allmendinger, R.W., T. E. Jordan, S. M. Kay, and B. L. Isacks, The evolution of the Altiplano-Puna plateau of the Central Andes, *Ann. Rev. Earth Planet. Sci.*, *25*, 139-174, 1997.

Angermann, D., J. Klotz, and C. Reigber, Space-geodetic estimation of the Nazca-South America Euler vector, *Earth Planet. Sci. Lett.*, *171*, 329-334, 1999.

Armijo, R., P. Tapponnier, J.L. Mercier, and T.L. Han, Quaternary extension in Southern Tibet: field observations and tectonic implications, *J. Geophys. Res.*, *91*, 13803-13872, 1986.

Baby, P., G. Herail, R. Salinas, and T. Sempere, Geometry and kinematic evolution of passive roof duplexes deduced from cross section balancing: Example from the foreland thrust system of the southern Bolivian subandean zone, *Tectonics*, *11*, 523-536, 1992a.

Baby, P., T. Sempere, J. Oller, and G. Herail, Evidence for major shortening on the eastern edge of the Bolivian Altiplano: The Calazaya nappe, *Tectonophysics*, *205*, 155-169, 1992b.

Bevis, M., E. Kendrick, R.J. Smalley, B. Brooks, R.W. Allmendinger, and B. Isacks, On the strenth of interplate coupling and the rate of back arc convergence in the central Andes: An analysis of the interseismic velocity field, *Geochemistry, Geophysics, Geosystems*, *2*, 2001GC000198, 2001.

Bourne, S.J., P.C. England, and B. Parsons, The motion of crustal blocks driven by flow of the lower lithosphere and implciations for slip rates of continental strike-slip faults, *Nature*, *391*, 655-659, 1998.

Cathles, L.M., *The viscosity of the Earth's mantle*, Princeton Press, Princeton, 1975.

Chen, Z., B.C. Burchfiel, Y. Liu, R.W. King, L.H. Royden, W. Tang, E. Wang, J. Zhao, and X. Zhang, Global positioning system measurements from eastern Tibet and their implications for India/ Eurasia intercontinental deformation, *J. Geophys. Res.*, *105*, 16,215-16,227, 2000.

Cladouhos, T.T., R.W. Allmendinger, B. Coira, and E. Farrar, Late Cenozoic deformation in the Central Andes; fault kinematics from the northern Puna, northwestern Argentina and southwestern Bolivia, *J. South Am. Earth Sci.*, *7*, 209-228, 1994.

Dalmayrac, B., and P. Molnar, Parallel thrust and normal faulting in Peru and constrains on the state of stress, *Earth Planet. Sci. Lett.*, *55*, 473-481, 1981.

DeMets, C., R.G. Gordon, D.F. Argus, and S. Stein, Effect of recent revisions to the geomagnetic reversal time scale on esti-

mates of current plate motion, *Geophys. Res. Lett.*, *21*, 2191-2194, 1994.

Desai, C.S., *Elementary finite element method*, 434 pp., Prentice-Hall, Englewood Cliffs, N. J., 1979.

Dewey, J.F., Extensional collapse of orogens, *Tectonics*, *7*, 1123-1139, 1988.

Dewey, J.F., and J. M. Bird, Mountain belts and the new global tectonics, *J. Geophys. Res.*, *75*, 2625-2647, 1970.

Dewey, J.F., and S.H. Lamb, Active tectonics of the Andes, *Tectonophysics*, *205*, 79-95, 1992.

Donnellan, A., B.H. Hager, and R.W. King, Discrepency between geological and geodetic deformation rates in the Ventura basin, *Nature*, *366*, 333-336, 1993.

Dragert, H., K. Wang, and T.S. James, A silent slip event on the deeper Cascadia subduction interface, *Science*, *292*, 1525-1528, 2001.

England, P.C., and D.P. McKenzie, A thin viscous sheet model for continental deformation, *Geophys. J. R. astr. Soc*, *70*, 295-321, 1982.

Flesch, L.M., A.J. Haines, and W.E. Holt, Dynamics of the India-Eurasia collision zone, *J. Geophys. Res.*, *106*, 16435-16460, 2001.

Flesch, L.M., W.E. Holt, A.J. Haines, and T.B. Shen, Dynamics of the Pacific-North American plate boundary in the Western United States, *Science*, *287*, 834-836, 2000.

Fukao, Y., A. Yamamoto, and M. Kono, Gravity anomaly across the Peruvian Andes, *J. Geophys. Res.*, *94*, 3867-3890, 1989.

Goetze, C., and B. Evans, Stress and temperature in the bending lithosphere as constrained by experimental rock mechanics, *Geophys. J. R. astr. Soc.*, *59*, 463-478, 1979.

Grange, F., P. Cunningham, J. Gagnepain, D. Hatzfeld, P. Molnar, L. Ocola, A. Rodrigues, S.W. Roecker, J.M. Stock, and G. Suarez, The configuration of the seismic zone and the downgoing slab in southern Peru, *Geophys. Res. Lett.*, *11*, 38-41, 1984.

Hindle, D., J. Kley, E. Klosko, S. Stein, T. Dixon, and E. Norabuena, consistency of geologic and geodetic displacements during Andean orogenesis, *Geophys. Res. Lett.*, in press, 2002.

Hodges, K.V., and J.D. Walker, Extension in the Cretaceous Sevier orogen, North American Cordillera, *Geol. Soc. Am. Bull.*, *104*, 560-590, 1992.

Holt, W., E., and A.J. Haines, Velocity fields in deforming Asia from the inversion of earthquake-related strains, *Tectonics*, *12*, 1-20, 1993.

Isacks, B.L., Uplift of the central Andean plateau and bending of the Bolivian orocline, *J. Geophys. Res.*, *93*, 3211-3231, 1988.

James, D.E., Plate-tectonic model for the evolution of the central Andes, *Geol. Soc. Am. Bull.*, *82*, 3325-3346, 1971.

Kendrick, E., M. Bevis, R.J. Smalley, and B. Brooks, An integrated crustal velocity field for the central Andes, *Geochemistry, Geophysics, Geosystems*, *2*, 2001GC000191, 2001.

King, R.W., F. Shen, B.C. Burchfiel, L.H. Royden, E. Wang, Z. Chen, Y. Liu, X. Zhang, J. Zhao, and Y. Li, Geodetic measurement of crustal motion in southwest China, *Geology, 25*, 179-182, 1997.

Kirby, S.H., and A.K. Kronenberg, Rheology of the lithosphere: Selected topics, *Rev. Geophys.*, *25*, 1,219-1,244, 1987.

Kley, J., C.R. Monaldi, and J.A. Salfity, Along-strike segmentation of the Andean foreland: causes and consequences, *Tectonophysics*, *301*, 75-94, 1999.

Lamb, S., Active deformation in the Bolivian Andes, South America, *J. Geophys. Res.*, *105*, 25,627-25,653, 2000.

Lambeck, K., Glacial rebound of the British Isles - II. A high-resolution, high-precision model, *Geophys. J. Int.*, *115*, 960-990, 1993.

Larson, K., R. Burgmann, R. Bilham, and J.T. Freymueller, Kinematics of the India-Eurasia collision zone from GPS measurements, *J. Geophys. Res.*, *104*, 1077-1094, 1999.

Leffler, L., S. Stein, A. Mao, T. Dixon, M. Ellis, L. Ocala, and I.S. Sacks, Constraints on the present-day shortening rate across the Central Eastern Andes from GPS measurements, *Geophys. Res. Lett.*, *24*, 1031-1034, 1997.

Liu, M., Y. Yang, S. Stein, Y. Zhu, and J. Engeln, Crustal shortening in the Andes: Why do GPS rates differ from geological rates?, *Geophys. Res. Lett., 27*, 3005-3008, 2000a.

Liu, M., Y. Shen, and Y. Yang, Gravitational collapse of orogenic crust: A preliminary three-dimensional finite element study, *J. Geophys. Res.*, *105*, 3159-3173, 2000b.

Lowry, A.R., and R.B. Smith, Strength and rheology of the western U. S. Cordillera, *J. Geophys. Res.*, *100*, 17,947-17,964, 1995.

Mercier, J.L., Extensional-compressional tectonics associated with the Aegean arc: Comparison with the Andean cordillera of south Peru-north Bolivia, *Philos. Trans. R. Soc. London*, *300*, 337-355, 1981.

Mercier, J.L., M. Sebrier, A. Lavenu, J. Cabrera, O. Bellier, J.-F. Dumont, and J. Machare, Changes in the tectonic regime above a subduction zone of Andean type: The Andes of Peru and Bolivia during the Pliocene-Pleistocene, *J. Geophys. Res.*, *97*, 11,945-11,982, 1992.

Molnar, P., and W.-P. Chen, Focal depths and fault plane solutions of earthquakes under the Tibetan plateau, *J. Geophys. Res.*, *88*, 1180-1196, 1983.

Molnar, P., and H. Lyon-Caen, Some simple physical aspects of the support, structure, and evolution of mountain belts, *Geol. Soc. Am. Special Paper*, *218*, 179-207, 1988.

Norabuena, E., L. Leffler-Griffin, A. Mao, T. Dixon, S. Stein, I.S. Sacks, L. Ocala, and M. Ellis, Space geodetic observations of Nazca-South America convergence along the Central Andes, *Science*, *279*, 358-362, 1998.

Norabuena, E.O., T.H. Dixon, S. Stein, and C.G.A. Harrison, Decelerating Nazca-South America and Nazca-Pacific plate motions, *Geophys. Res. Lett.*, *26*, 3405-3408, 1999.

Pope, D.C., and S.D. Willett, Thermal-mechanical model for crustal thickening in the central Andes driven by ablative subduction, *Geology*, *26*, 511-514, 1998.

Ranalli, G., *Rheology of the Earth*, 413 pp., Chapman & Hall, London, 1995.

Roy, M., and L.H. Royden, Crustal rheology and faulting at strike-slip plate boundaries; 1, An analytic model, *J. Geophys. Res.*, *105*, 5583-5597, 2000a.

Roy, M., and L.H. Royden, Crustal rheology and faulting at strike-slip plate boundaries; 2, Effects of lower crustal flow, *J. Geophys. Res.*, *105*, 5599-5613, 2000b.

Russo, R.M., and P.G. Silver, Cordillera formation, mantle dynamics, and the Wilson cycle, *Geology*, *24*, 511-514, 1996.

Savage, J.C., A dislocation model of strain accumulation and release at a subduction zone, *J. Geophys. Res.*, *88*, 4984-4996, 1983.

Sbar, M.L., An explanation for contradictory geodetic strain and fault plane solution data in western North America, *Geophys. Res. Lett.*, *10*, 177-180, 1983.

Schmitz, M., A balanced model of the southern Central Andes, *Tectonics*, *13*, 484-492, 1994.

Sebrier, M., J.L. Mercier, F. Megard, G. Laubacher, and E. Garey-Gailhardies, Quaternary normal and reverse faulting and the state of stress in the central Andes of south Peru, *Tectonics*, *4*, 87-105, 1985.

Sella, G.F., T. Dixon, and A. Mao, REVEL: A model for recent plate velocities from space geodesy, *J. Geophys. Res.*, in press, 2002.

Sheffels, B., Lower bound on the amount of crustal shortening in the central Bolivian Andes, *Geology*, *18*, 812-815, 1990.

Somoza, R., Updated Nazca (Farallon)-South America relative motions during the last 40 Myr: implications for mountain building in the central Andean region, *J. South Amer. Earth Sci.*, *11*, 211-215, 1998.

Suarez, G., P. Molnar, and B.C. Burchfiel, Seismicity, fault plane solutions, depth of faulting, and active tectonics of the Andes of Peru, Ecuador, and southern Colombia, *J. Geophys. Res.*, *88*, 10403-10428, 1983.

Walcott, R.I., Flexual rigidity, thickness and viscosity of the lithosphere, *J. Geophys. Res.*, *75*, 3941-3954, 1970.

Wang, K., Stress-strain "paradox", plate coupling, and forearc seismicity at the Cascadia and Nankai subduction zones, in *Seismic structure and stress regime of subduction zones; selected papers*, edited by D. Zhao, and A. Hasegawa, Elsevier. Amsterdam, Netherlands. 2000., 2000.

Wernicke, B., A.M. Friedrich, N.A. Niemi, R.A. Bennett, and J.L. Davis, Dynamics of plate boundary fault systems from Basin and Range Geodetic Network (BARGEN) and geological data, *GSA Today*, *10*, 1-7, 2000.

Williams, C.A., and R.M. Richardson, A rheological layered three-dimensional model of the San Andreas Fault in central and southern California, *J. Geophys. Res.*, *96*, 16597-16623, 1991.

Yang, Y., and M. Liu, Deformation of convergent plates: Evidence from discrepancies between GPS velocities and rigid-plate motions, *Geophys. Res. Lett.*, in press, 2002.

Yin, A., and M. Harrison, Geological Evolution of the Himalayan-Tibetan orogen, *Ann. Rev. Earth. Planet. Sci.*, *28*, 211-280, 2000.

Zandt, G., S.L. Beck, S.R. Ruppert, C.J. Ammon, D. Rock, E. Minaya, T.C. Wallace, and P.G. Silver, Anomalous crust of the Bolivian Altiplano, Central Andes: constraints from broadband regional seismic waveforms, *Geophys. Res. Lett.*, *23*, 1159-1162, 1996.

_____

Mian Liu and Youqing Yang. 101 Geological Sciences Building, Columbia, Missouri, 65211. (lium@missouri.edu)

Seth Stein and Eryn Klosko. Dept. of Geological Sciences, Northwestern University, Evanston, Illinois, 60208. (seth@earth.northwestern.edu)